Chemical Science

RSC Publishing

EDGE ARTICLE

View Article Online
View Journal | View Issue

Cite this: *Chem. Sci.*, 2013, **4**, 3731

Delivery and release of curcumin by a hypoxia-activated cobalt chaperone: a XANES and FLIM study†

Anna K. Renfrew,* Nicole S. Bryce and Trevor W. Hambley

Received 31st May 2013
Accepted 10th July 2013

DOI: 10.1039/c3sc51530c

www.rsc.org/chemicalscience

We present a bioreductively activated cobalt(III) carrier system for the delivery of curcumin with enhanced drug stability, tumour penetration and efficacy in hypoxic tumour regions. Curcumin is a natural product with potent anticancer activity but low bioavailability and serum stability. With the aim of overcoming these limitations, we prepared a cobalt(III) prodrug of curcumin and compared the stability, cytotoxicity and cellular uptake with those of the free drug. Using a combination of fluorescence lifetime imaging and X-ray absorption spectroscopy, we demonstrated that curcumin is released from the cobalt carrier complex in tumour cells, with strong evidence to suggest that the process occurs *via* reduction of the cobalt centre. Furthermore, fluorescence lifetime imaging in solid tumour models showed that the cobalt complex delivered curcumin uniformly throughout the tumour model, while free curcumin only accumulated on the outer edges. For comparison, we also investigated the isoelectronic ruthenium(II) complex and found its properties and biological activity to be very different to those of the cobalt analogue.

Introduction

The efficacy of many anticancer therapeutics is compromised by poor stability, solubility and selectivity for tumour cells. A viable strategy to overcome these limitations is through complexation of the drug to a metal complex. Transition metal complexes are particularly suitable as tumour-selective drug delivery agents, having metal–ligand bond that are highly responsive to environmental factors such as pH, redox, light and temperature. A range of rationally designed, metal-based drug carriers have been reported in recent years, including bioreductive drug chaperones,[1,2] light-activated prodrugs[3,4] and metallo-cages that can exploit the EPR effect for the transport of small hydrophobic molecules.[5] An understanding of the stability, distribution and fate of both the metal and cytotoxin in a cellular system is key to evaluating the efficacy of prodrugs and chaperone complexes, but current methods are limited and often do not provide a complete picture. Metal accumulation studies will confirm whether a complex enters the cell but do not give any information on oxidation state or coordination environment. Similarly, fluorescent tags can be employed to monitor cellular localisation by confocal fluorescence microscopy but in most cases this does not show whether the metal–drug complex remains intact.

Research within our group and others has shown synchrotron radiation to be an effective way of determining both the oxidation state and coordination sphere of metal complexes in tumour cells.[6–8] This technique is particularly useful for monitoring the activation of bioreductive prodrugs such as platinum(IV) and ruthenium(III) as reduction of the metal centre can be observed but it does not give any information on the fate of the cytotoxin. Fluorescent cytotoxins can be visualised in cells by fluorescence microscopy, but this technique gives limited information on whether the cytotoxin is still bound to the metal centre. Fluorescence lifetime imaging (FLIM) is a powerful tool for monitoring fluorescent drugs in cellular systems and is widely used to study small molecule fluorophores,[9–11] though the use of FLIM to study metal complexes *in vitro* has been limited to ruthenium and rhenium polypyridyl oxygen sensors and bis(thiosemicarbazone) radio metal complexes.[12,13] Here we use a combination of X-ray absorption spectroscopy and fluorescence lifetime imaging to evaluate the cellular uptake, distribution and fate of novel metal curcumin complexes in tumour cells.

The natural product, curcumin, isolated from *curcuma longa* (turmeric), exhibits potent activity in cell culture and animal studies, acting as an anti-proliferative, anti-metastatic and anti-angiogenic agent.[14] However, clinical use of curcumin as an anticancer agent has met with limited success. Poor solubility and rapid metabolism result in very low bioavailability upon oral administration. Daily doses of 8–12 g of curcumin were found to give a plasma concentration of less than 1 $\mu g\ mL^{-1}$, far lower than the level required for a significant pharmacological effect.[15,16] A large number of synthetic curcuminoids have been prepared with the aim of overcoming these limitations, though these often require many synthetic steps.[17] An alternative strategy to improving the properties of curcumin, without the

School of Chemistry, University of Sydney, Sydney, Australia. E-mail: anna.renfrew@sydney.edu.au; Fax: +61 2 9351 3329; Tel: +61 2 9351 4233

† Electronic supplementary information (ESI) available. See DOI: 10.1039/c3sc51530c

need to modify the drug, is the incorporation of curcumin into delivery vehicles and a number of possible macromolecular carriers, including nanoparticles, micelles and micro-emulsions, have been evaluated in recent years.[18]

Our interest has focused on cobalt(III)[19,20] complexes as bio-reductive drug chaperones. Coordination to inert cobalt(III) deactivates a cytotoxin under normal physiological conditions; however, in the presence of a large excess of reducing agents and an oxygen deficient environment, such as found in a hypoxic tumour, the cobalt(III) centre is reduced to labile cobalt(II) and the cytotoxin released.[21] We have previously demonstrated that cobalt(III) complexes are suitable hypoxia-selective chaperones for carboxylic[22] and hydroxamic[23] acid containing drugs, including the matrix metalloproteinase inhibitor Marimastat.[24] Here we evaluate two potential metal chaperone complexes for the delivery and release of curcumin, a cobalt(III) complex and the isoelectronic ruthenium(II) analogue. Ruthenium(II) complexes are gaining increasing attention as potential anticancer agents, with a number showing high selectivity towards cancer cells.[25] While several metal–curcumin complexes with anti-alzheimers[26,27] or anticancer[28,29] properties have been reported previously, to the best of our knowledge none have focused on the delivery and release of curcumin in tumour cells and tumour models.

Results and discussion

Syntheses of the complexes

Curcumin contains a 1,3 diketone moiety and coordinates metal complexes as a 1,3 β-hydroxyketone.[30] Ruthenium and cobalt complexes of curcumin and related diketone ligands acetylacetone (acac) and dibenzoylmethane (dbm), were prepared with tris(2-methylpyridine)amine (tpa) as the ancillary ligand (Fig. 1). tpa was chosen as it is known to form highly stable complexes with both ruthenium[31] and cobalt[23] and the reduction potential of cobalt(III)–tpa complexes has previously been established to be within a biologically relevant window. All complexes were obtained in good yield by refluxing $[MCl_2(tpa)]ClO_4$ in water with 1 equivalent of the protonated acac ligand and 1.2 equivalents of triethylamine. Addition of excess $NaClO_4$ induced precipitation of the product as monocationic (**1a–c**) or dicationic (**2a–c**) perchlorate salts. The complexes are highly soluble in polar organic solvents and sparingly to moderately soluble in water. All complexes were characterised by ^{1}H NMR, IR and UV-vis spectroscopy, ESI-mass spectrometry, elemental analysis and **1a**, **1b** and **2b** by X-ray crystallography (ESI†).

Each of the structures exhibits a distorted octahedral structure with bond lengths typical of those described in the literature for related ruthenium(II)[31] and cobalt(III)–tpa complexes.[32] For ruthenium complexes **1a** and **1b**, the metal–nitrogen bonds lengths are similar to the metal–oxygen bond lengths, while for cobalt complexes **2a** and **2c**, the metal–oxygen bond lengths are notably shorter. ORTEP plots derived from the X-ray crystal structures of complexes **1a**, **1b** and **2b** are given in Fig. 2 and selected bond lengths are listed in Table 1, with those of **2a** included for comparison.

Electrochemistry

Cyclic voltammograms in DMF were obtained for all complexes (Table S1 ESI†). While the acac and dbm complexes have only a single peak corresponding to a one electron oxidation or reduction on the metal centre, the curcumin complexes **1c** and **2c** also show a reduction of the ligand at −1560 mV *vs.* Fc/Fc^+.[33] Ruthenium complexes **1a–1c** undergo a one electron oxidation around −200 mV corresponding to the Ru(II)/(III) couple. These processes ranged from almost fully reversible for **1a**, to quasi-reversible for **1b**, to irreversible for **1c**. Cobalt complexes **2a–c** show a one electron reduction at −650 to −950 mV corresponding to the Co(II)/(III) couple. As for the ruthenium complexes, the process was almost reversible for **2a**, quasi-reversible for **2b**, and irreversible for **2c**.

Characterisation in solution

The fluorescence properties of curcumin complexes **1c** and **2c** were compared to those of the free ligand. While curcumin is strongly fluorescent in many organic solvents, the fluorescence quantum yield is solvent-dependent and is only around 0.01 in

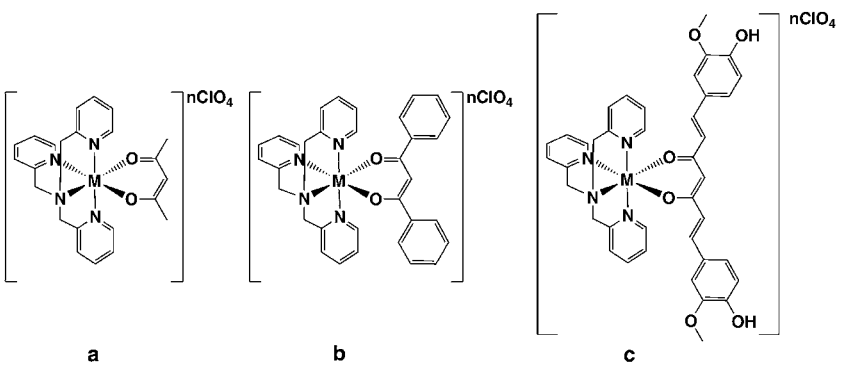

Fig. 1 Chemical structures of ruthenium and cobalt complexes prepared.

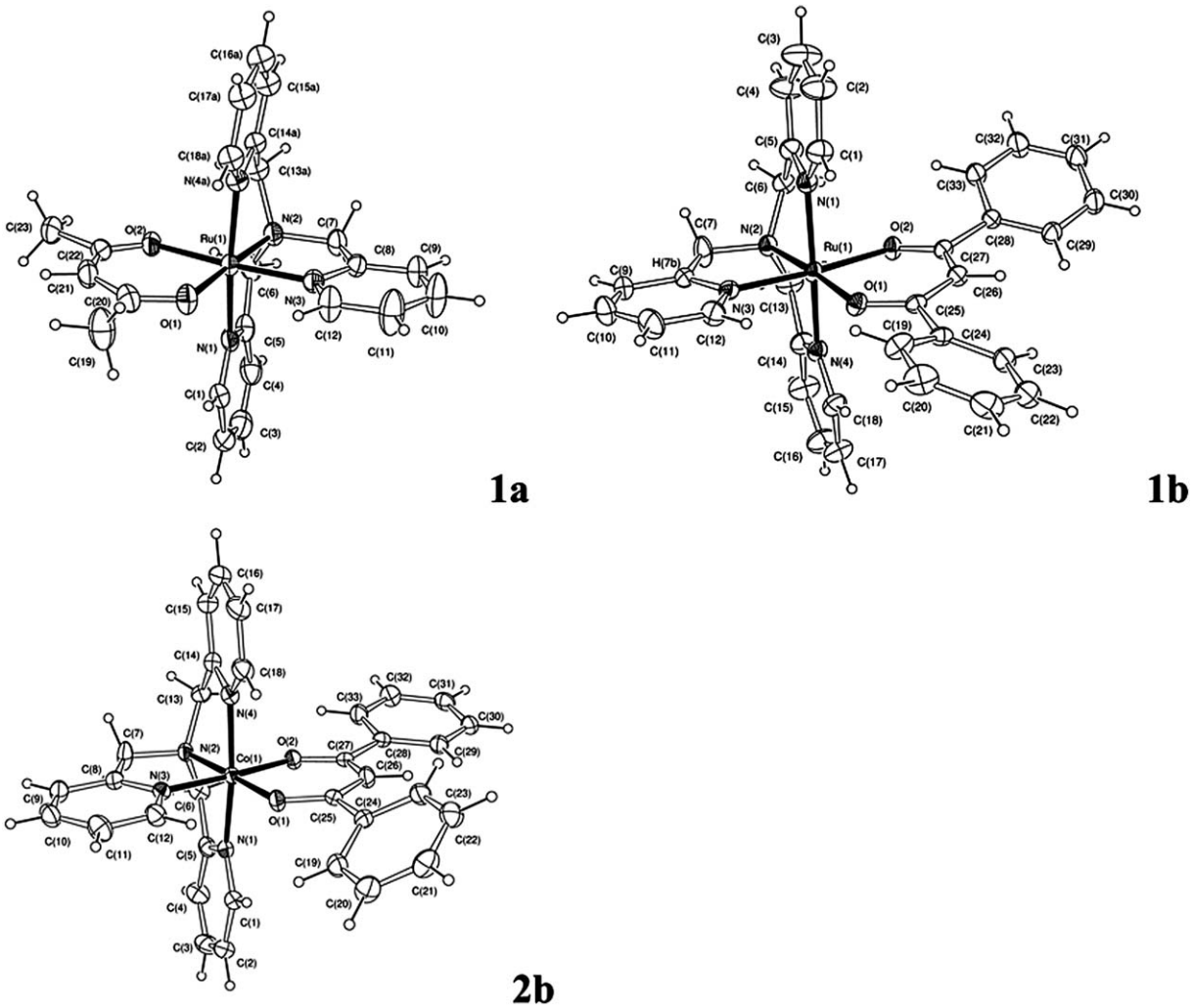

Fig. 2 ORTEP plots of **1a**, **1b** and **2b** with non-hydrogen atoms represented by thermal parameters with 50% probability ellipsoids. ClO_4 counter anions have been omitted for clarity.

Table 1 Comparison of selected bond lengths (Å) and angles (°) of complexes

	1a	1b	2a[a]	2b
M-O1	2.040(8)	2.0592(8)	1.8847(14)	1.8794(19)
M-O2	2.063(2)	2.0637(8)	1.9027(14)	1.886(2)
M-N1	2.061(3)	2.0537(11)	1.9304(17)	1.918(2)
M-N2	2.056(3)	2.0621(9)	1.9510(17)	1.943(2)
M-N3	2.025(3)	2.0305(10)	1.9240(18)	1.920(2)
M-N4	2.040(8)	2.0520(11)	1.9281(18)	1.926(3)

[a] From ref. 32.

aqueous solution.[34] Though emission was also significantly quenched in buffer/DMSO solutions, we observed that a reasonable emission spectrum could be obtained in TRIS buffer solution (pH 7.4) with 4% methanol (Fig. 3a). Under the same conditions, the curcumin emission from complexes **1c** and **2c** is quenched to *ca.* 10% of that of the free fluorophore. A number of d^6 transition metals, including ruthenium(II)[35,36] and cobalt(III),[22] have been reported to quench the fluorescence of coordinated fluorophores through energy or electron transfer processes. This effect provides a convenient means of observing fluorophore release by the increase in fluorescence, both in solutions and in live cells.

In order to determine the stability of the complexes under pseudo-physiological conditions, the emission spectra of **1c** and **2c** in TRIS buffer (pH 7.4) were measured at regular intervals over 20 hours. Neither complex showed any increase in fluorescence over the measured time, which suggests that the curcumin ligand remains coordinated (Fig. 3c, S1, ESI†). To evaluate the stability of the complexes towards biological reductants, the TRIS buffer solutions were treated with 10 equivalents of ascorbic acid or glutathione and the fluorescence emission monitored over the same time period (Fig. 3b and c, S1, ESI†). For complex **1c**, only a 2-fold increase in fluorescence was observed in the presence of ascorbic acid and 3-fold increase in the presence of glutathione (Fig. S1, ESI†). This result was expected for ascorbic acid as the ruthenium(II) complex is resistant to reduction. However, many ruthenium(II) complexes are known to react readily with glutathione.[19,20]

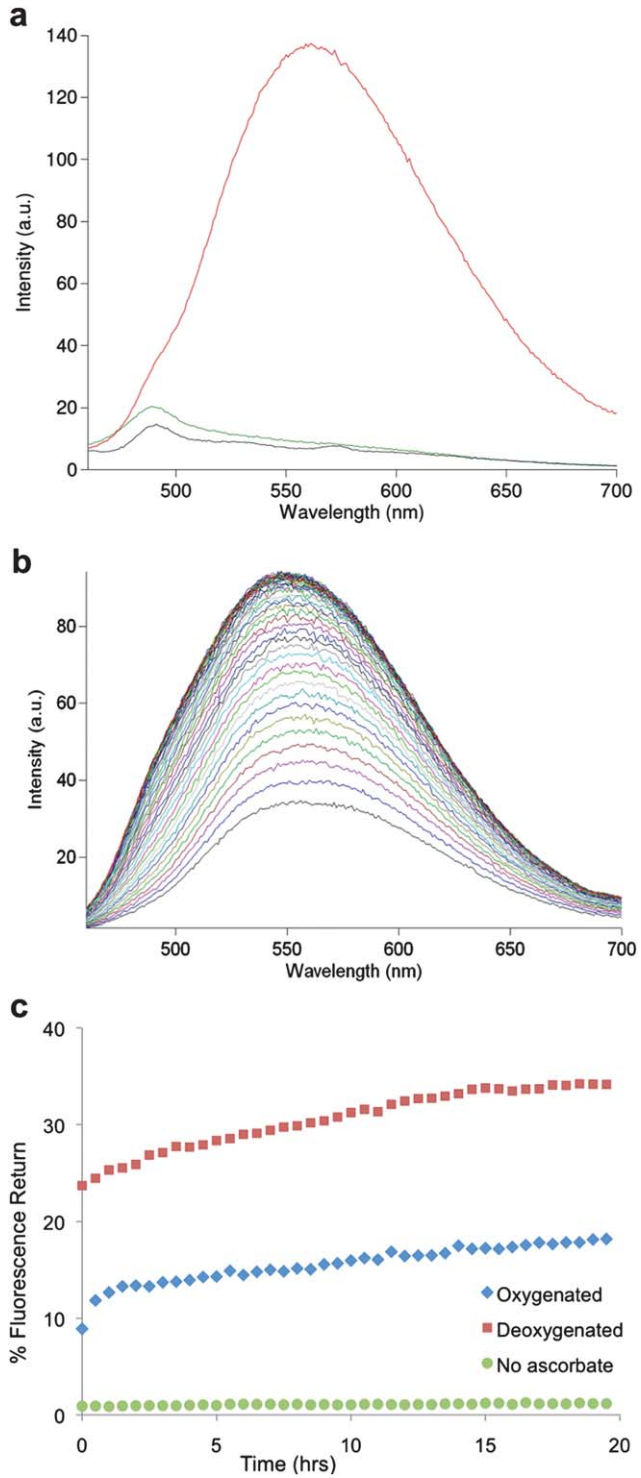

Fig. 3 (a) Absorbance and emission spectra of curcumin (red), **1c** (green) and **2c** (purple) λ_{ex} = 420 nm. (b) Increase in emission over time of a deoxygenated solution of **2c** with excess ascorbic acid. (c) Comparison of fluorescence return traces for **2c** with excess ascorbic acid in deoxygenated and oxygenated solutions, and in the absence of reducing agent.

Repeating the experiment in deoxygenated solutions did not affect the extent of fluorescence return. While **2c** also showed minimal fluorescence increase when treated with glutathione (Fig. S1, ESI†), in the presence of ascorbate the fluorescence intensity increased to 18% of that of free curcumin. When the experiment was repeated in a deoxygenated solution, the extent of fluorescence return doubled to 36% (Fig. 3c). This preferential ligand release under reducing and oxygen-free conditions is consistent with a reductive mechanism of activation.

Cytotoxicity

The cytotoxicities of all complexes and free acac ligands were evaluated against the colorectal cancer cell line DLD-1 and are summarised in Table 2. This cell line was chosen as curcumin is currently undergoing Phase I/II clinical trials against colorectal cancer. The IC_{50} value determined for curcumin is in agreement with that previously reported in the same cell line.[37] IC_{50} values were found to be dependent on both the nature of the metal and the acac ligand. For ruthenium complexes **1a–1c**, the trend curcumin > acac > dbm was observed. The same trend has been reported for the [Ru(*p*-cymene)(acac)Cl] series in the A2780 ovarian cancer cell line and was attributed to lipophilicity.[29,38] For **1a** and **1b** in particular, the complex is more cytotoxic than either the free acac ligand or $[RuCl_2(tpa)]ClO_4$ by more than factor of 10.

In contrast, for cobalt complexes **2a–c**, the IC_{50} values were consistently higher than those of the free acac ligands, implying that the cobalt–tpa moiety does not induce any cyototoxic effects of its own. Furthermore, the dichlorido precursor complex, $[CoCl_2(tpa)]ClO_4$, exhibited no toxicity up to a concentration of 200 μM. The trend IC_{50} acac > curcumin > dbm mirrors that of the free acac ligands, suggesting that cell death may result from release of the ligands and not from toxicity of the cobalt complex. High IC_{50} values are typical of this class of cobalt-chaperone where any effect is thought to be due to release of a cytotoxin rather than the complex itself.[21]

Fluorescence confocal microscopy in monolayer and 3-dimensional cell culture

To evaluate the effect of complexation on curcumin localisation, the fluorescence distribution of free curcumin, **1c** and **2c**, in both monolayer cells and spheroids was imaged. Spheroids (three-dimensional aggregates of tumour cells) are excellent models of solid avascular tumours as they display many of the same characteristics, including concentration gradients of

Table 2 IC_{50} values determined in DLD-1 colon cancer cells

Complex	IC_{50} (μM)
1a	5 ± 2
1b	1.6 ± 0.2
1c	52 ± 8
2a	>200
2b	29 ± 2
2c	39 ± 4
acac	>200
dbm	19 ± 1
Curcumin	13 ± 2
$[RuCl_2(tpa)]ClO_4$	>200
$[CoCl_2(tpa)]ClO_4$	>200

oxygen and biochemical waste products, areas of hypoxia and necrosis, and similar drug diffusion profiles.[39,40]

2-Dimensional monolayer cell culture

In DLD-1 cells treated with free curcumin for 24 h, the fluorophore was found to have a preferential localisation in membraneous structures, with fluorescence observed almost uniquely in the membranes of cytoplasmic organelles and the nuclear membrane (Fig. 4). The cytoplasmic staining pattern was similar to that seen in DLD-1 cells stained with Mitotracker (Fig. S2, ESI†). Curcumin accumulation in cellular membranes, and to a lesser extent in nuclear membranes, has previously been observed in MCF-7 (breast cancer) and NIH3T3 (fibroblast) cells,[41] while accumulation in the cytoplasm was reported for HeLa (cervical cancer) cells.[28] It should be noted that the quantum yield of fluorescence emission for curcumin is significantly higher in hydrophobic environments, such as membraneous structures, therefore the possibility that curcumin is also accumulating in other regions of the cell, where its fluorescence is quenched, cannot be ruled out. Complexes **1c** and **2c** showed very similar fluorescence distributions to those of free curcumin though the intensity was considerably lower. Importantly, this demonstrates that coordination to the metal complexes does not prevent the cellular uptake of curcumin.

3-Dimensional spheroid cell culture

Fluorescence confocal microscopy images of spheroids treated with curcumin, **1c** and **2c** for 24 h are shown in Fig. 5a–c. The fluorescence distribution patterns of the treated spheroids were found to be markedly different for the complexes compared to the free drug. While fluorescence for the curcumin treated sample was observed only on the periphery of the spheroid, considerable fluorescence was observed throughout the spheroids following treatment with **1c** and **2c**. Previous work within our group has found that charged complexes exhibit significantly better penetration through spheroids than neutral complexes or free ligands.[39] This is thought to be due to the slower uptake of the charged complexes allowing greater diffusion between the cells, so that a higher proportion of the drug can reach the central regions of the spheroid. In particular, **2c** shows high levels of accumulation throughout the central regions of the spheroid that have been previously been determined to be hypoxic (70–150 μm from the periphery).[39,42] There is considerable interest in drugs that can penetrate as far as the hypoxic regions, as these cells are typically highly aggressive and drug resistant, and among the most difficult to treat.[43] The fluorescence of the **1c**-treated sample is limited to the periphery and the most central region of the spheroid, where cells are generally necrotic (>150 μm from the periphery).

To confirm that the observed fluorescence did not result from metabolites of the metal complexes, spheroids treated with $[RuCl_2(tpa)]ClO_4$ and $[CoCl_2(tpa)]ClO_4$ were imaged under the same conditions but no fluorescence was observed for either complex (Fig. S3, ESI†). In both monolayer cells and spheroids, the fluorescence intensity of **1c** and **2c** was significantly lower than that of free curcumin. From the solution emission spectra recorded at pH 7.4 (Fig. 3a) it is clear that fluorescence of curcumin is significantly quenched on complexation, however both **1c** and **2c** are slightly fluorescent in the same region as curcumin ($\lambda_{em\ max} = 500$ nm). To limit the possibility of fluorescence from the intact complexes, confocal microscopy images were collected in the range 540–800 nm, where fluorescence from **1c** and **2c** is minimal (Fig. 3a). However, it could not be conclusively determined whether the cellular fluorescence observed resulted from a low concentration of free curcumin or a higher concentration of complexed curcumin. In order to distinguish between free and complexed curcumin, we used fluorescence lifetime imaging (FLIM), using the difference in the fluorescence lifetimes to establish whether the curcumin was metal bound.

Fluorescence lifetime imaging in 3-D spheroid tumour models

The average lifetime of fluorescence for curcumin, **1c** and **2c** were measured in cell free (methanol) solutions and live cells (average values shown in Table 3). As has previously been reported, the fluorescence lifetime of free curcumin could not be determined in methanol as it is shorter than the instrument response time of 130 ps,[44] however, fluorescence lifetime values for both **1c** and **2c** in methanol could be measured. All FLIM experiments involving live cells were performed in spheroids, due to the low fluorescence levels of **1c** and **2c**. Images of monolayer cells with high magnification objectives could not be obtained as the level of laser power required to obtain sufficient numbers of measurable photons over the relatively small area within the short timeframe necessary to avoid cell movement artefacts, destroyed the samples. In contrast, as spheroids were imaged at a lower magnification, the laser power and time

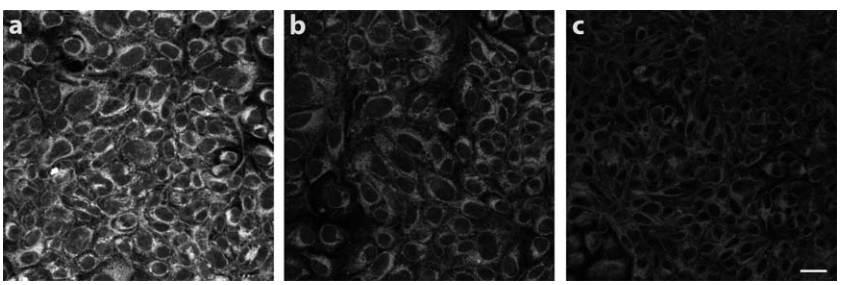

Fig. 4 DLD-1 cells treated with 20 μM of curcumin (a), **1c** (b) and **2c** (c). Scale bar = 20 μm.

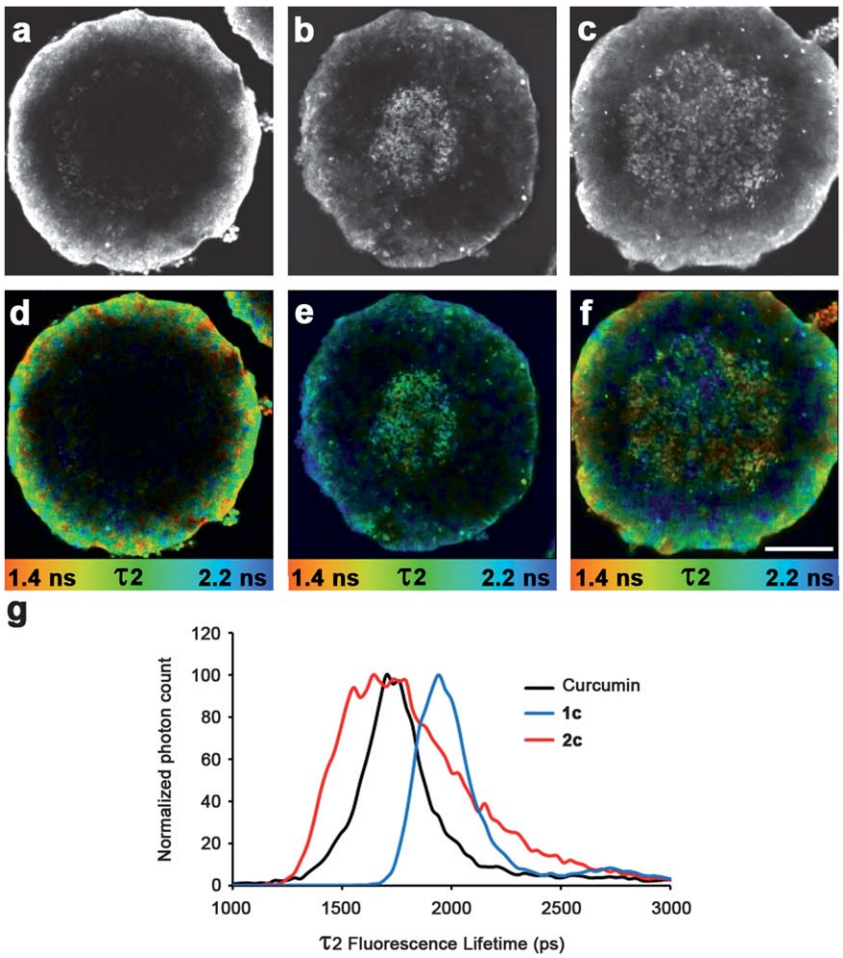

Fig. 5 Top: confocal fluorescence microscopy images of spheroids treated with 20 μM of (a) curcumin (b) **1c** and (c) **2c**. Middle: lifetime maps of the treated spheroids (d) curcumin (e) **1c** (f) **2c** (scale bar = 100 μm). Bottom: (g) global lifetime emissions for curcumin, **1c** and **2c**.

Table 3 Fluorescence lifetime values of curcumin, **1c** and **2c**[a]

	τ1 (ps)	τ2 (ps)	A1 (%)	A2 (%)	χ^2
Cell free					
Curcumin	nd	nd			
1c	353 ± 32	2598 ± 52	58	42	1.02
2c	650 ± 27	2920 ± 45	57	43	1.01
Spheroid culture					
Curcumin	419 ± 12	1675 ± 55	71	29	1.01
1c	431 ± 17	2124 ± 32	72	28	1.01
2c	408 ± 18	1751 ± 32	72	28	1.02

[a] nd = not determinable.

required to obtain a sufficient number of measurable photons was achievable without sample destruction. These images provide an overall view of where the compounds are located but lack the precise intra/intercellular detail required to determine cellular localisation.

The lifetime of curcumin in methanol is extremely short and below the system response time of 130 ps, through a two component process with τ1 = 12 ps and τ2 = 70 ps measured by ultrafast fluorescence upconversion, has previously been reported.[45] The fluorescence decay of **1c** and **2c** in methanol was also found to proceed *via* a two-component process, with considerably longer lifetimes than the free ligand (Table 3). τ2 components were similar for the two complexes, while τ1 is markedly shorter for **1c** (353 *vs.* 650). In the cellular system, the fluorescence decay curve of curcumin required a biexponential fit. For **1c** and **2c** in a cellular system, there is the possibility of a four-component decay due to the presence of both complexed and uncomplexed curcumin; however, in each case the data could be fitted to a biexponential decay. Curcumin and both complexes were found to have similar τ1 values, whereas significant variations in the distribution and length of the τ2 component were observed (Fig. 5g).

In the case of the **1c**-treated spheroids, there is little difference in either the τ1 or τ2 components between the methanol and cellular samples. The τ2 component is also significantly longer than that of the samples dosed with free curcumin. Both observations suggest that ruthenium–curcumin complex remains largely intact, in agreement with the unusual stability of the complex under pseudo-physiological solution discussed above. However, while the average τ2 component of the **1c**-treated spheroid is notably longer than that of curcumin, it is clear from the false colour image (Fig. 5e) that there is a difference in

lifetime between the periphery and central region of the spheroid. The longest lifetimes are observed on the periphery in blue, with a shift towards shorter lifetimes in the centre, which may indicate that the complex remains intact in the outer region of the spheroid, but a percentage is metabolised in the central region. For complex **2c**, both the $\tau 1$ and $\tau 2$ values are almost halved on moving from the methanol solutions to the spheroid sample. Furthermore, the t2 component for **2c**-treated spheroids was found to be very close to that of free curcumin, suggesting that the ligand has at least partly dissociated. The false colour images of the $\tau 2$ lifetime component in treated spheroids show the similar lifetime distribution profiles of curcumin and **2c** (Fig. 5d and f). The broad distribution of the average $\tau 2$ lifetime for **2c** treated spheroids (Fig. 5g) may be due to the presence of both complexed and uncomplexed curcumin, suggesting that curcumin release is incomplete. This effect can also be observed in the false colour lifetime image (Fig. 5f) and may be a consequence of the continual diffusion of compound into the spheroid from the media. A recent study by Waghorn *et al.* reported a similar observation, where the combination of both the free ligand and complex in cellular systems resulted in a broad distribution of fluorescent lifetimes.[12] However, unlike the **1c**-treated sample, the broad distribution of lifetimes is consistent in all regions of the spheroid. This indicates that there is a mixture of free and bound curcumin throughout the spheroid, and significantly, that curcumin is being released in the hypoxic and necrotic regions of the spheroid as well as on the periphery.

X-ray absorption studies in DLD-1 cells

To establish whether curcumin release from **2c** occurs through ligand exchange or reduction of the cobalt(III) prodrug, XANES studies were carried out on DLD-1 cells treated with **2c**. We have previously demonstrated the use of XANES to probe the oxidation state of both platinum and cobalt complexes in tumour cell samples. There are a number of characteristic features in the K-edge spectra of cobalt(II) and cobalt(III) complexes that allow the oxidation state of a complex to be assigned.[46] The XANES spectra of cobalt(II) complexes are independent of coordination environment and have a single absorption peak at *ca.* 7723 eV and post-edge minimum around 7750 eV. In contrast, cobalt(III) spectra vary considerably depending on the nature of the ligand sphere. Cobalt(III) complexes have a major absorption peak at lower energies, at *ca.* 7727 eV, and a neighbouring peak around 7740 eV, with post-edge minima between 7757 and 7762 eV.[47,48] While peak heights vary with coordination environment, the edge energies for cobalt(II) complexes are consistently higher than for cobalt(III) complexes.

The XANES spectra of **2c**, cells incubated with **2c** for 4 hours, and possible metabolites of **2c** are shown in Fig. 6. The chemical structures of the possible metabolites studied are listed in Fig. 6 (top). Cobalt chloride was used as a cobalt(II) standard. The cobalt(III) metabolites are possible products of aquation (**3**) or reaction with cysteine (**5–7**). Previous studies into cobalt(III) complexes conducted in both solutions and biological systems have shown the tris–cysteine complex **7**, or similar complexes, to be the major metabolite, in some cases *via* the intermediate **5**. The spectrum of **2c** is typical of a cobalt(III) complex and very similar to those previously reported for related cobalt(III)–tpa compounds with hydroxamate or nitrate ligands.[46,47] In the case of the sulphur-coordinated complexes **5**, **6** and **7**, the edge energies are notably lower than those of the other cobalt(III) complexes (*ca.* 7720 eV *vs.* 7727 eV). This effect has been reported previously for cobalt and other metal complexes and is attributed to the high covalency of metal–sulphur bonds.[49]

After incubation of **2c** in cells for 4 hours, there are marked differences in the XANES spectrum. The spectrum of the cell sample is characteristic of cobalt(II), with a shift to higher energy of both the major absorption peak and post-edge minimum, and loss of the second absorption peak. Comparison with the spectra of complexes **3–7** shows that the cell sample trace overlays very closely with the cobalt(II) standard **4**,

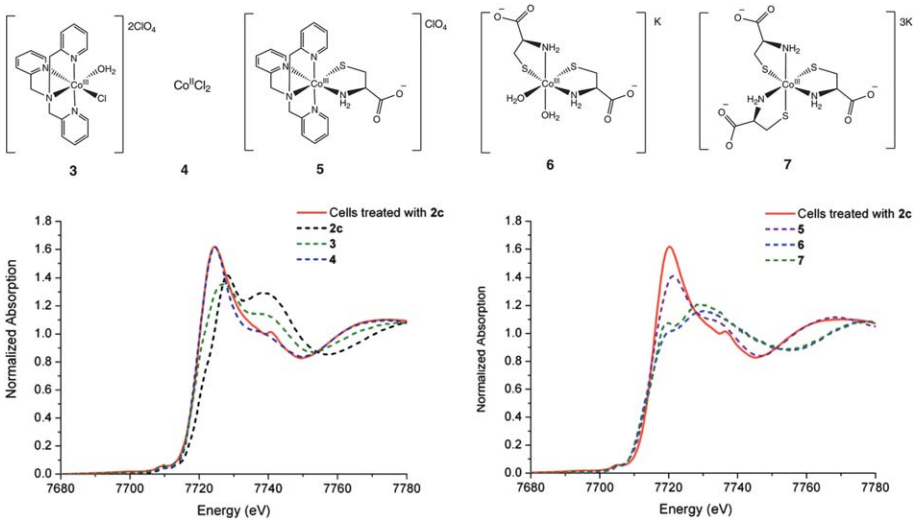

Fig. 6 Top: chemical structures of complexes **3–7**. Bottom left: XANES spectra of DLD-1 cells treated with **2c** (red), **2c** and aquation product **3** and cobalt(II) standard **4**. Bottom right: XANES spectra of DLD-1 cells treated with **2c** (red), with possible cobalt(III) cysteine metabolites **5**, **6** and **7**.

indicating that the majority of the complex has been reduced after 4 hours incubation. This result, in combination with the fluorescence return studies performed under anaerobic conditions, suggests that reduction to cobalt(II) is involved in the mechanism of curcumin release from **2c**.

Conclusions

In conclusion, we have demonstrated that the cobalt chaperone complex **2c** is suitable for the delivery and release of curcumin. Incorporation of curcumin into the cobalt(III) chaperone was found to improve stability and solubility in aqueous solutions, and to enhance tumour penetration and uptake into hypoxic and necrotic regions. The fluorescence studies conducted in the presence of reducing agents, and X-ray absorption studies in tumour cells, both suggest that curcumin release occurs *via* reductive activation of the prodrug to cobalt(II). This is a potential means of significantly improving the efficacy of curcumin in hypoxic tumour regions, both through increasing penetration of the prodrug to hypoxic regions and by preferential release of the drug in a reducing environment.

The ruthenium complex **1c** was found to be considerably more stable than its cobalt analogue, with little curcumin release observed either in solution or in cells. While this remarkable stability means that the complex is not possibly suitable for curcumin delivery, the low IC_{50} values of the other ruthenium analogues **1a** and **1b** suggest that this class of compounds induce cell death by a different mechanism to that of the cobalt complexes and may merit further studies.

While this work has focused on curcumin complexes, the techniques used to evaluate stability and distribution could be applied to any chaperone complex containing a fluorescent ligand or intrinsically fluorescent metal complex. In particular, FLIM was shown to be a valuable tool for monitoring the distribution and fate of the fluorescent ligand and complexes. Such information is very important to the future design of this promising class of drug chaperone complexes.

Acknowledgements

The authors acknowledge scientific and technical input and support from the Australian Microscopy & Microanalysis Research Facility (AMMRF) node at the University of Sydney. XANES studies were was performed at the Australian National Beamline Facility with support from the Australian Synchrotron Research Program, which was funded by the Commonwealth of Australia under the Major National Research Facilities Program. The authors acknowledge Dr Julia Norman and Dr Jenny Zhang for help with the XANES studies. We thank the Australian Research Council for support through ARC Discovery Grant DP110100461 and the Swiss National Science Foundation for a postdoctoral fellowship (akr).

Notes and references

1 D. C. Ware, B. D. Palmer, W. R. Wilson and W. A. Denny, *J. Med. Chem.*, 1993, **36**, 1839–1846.
2 P. J. Blower, J. R. Dilworth, R. I. Maurer, G. D. Mullen, C. A. Reynolds and Y. F. Zheng, *J. Inorg. Biochem.*, 2001, **85**, 15–22.
3 T. Respondek, R. N. Garner, M. K. Herroon, I. Podgorski, C. Turro and J. J. Kodanko, *J. Am. Chem. Soc.*, 2011, **133**, 17164–17167.
4 C. C. L. Zayat, P. Albores, L. Baraldo and R. Etchenique, *J. Am. Chem. Soc.*, 2003, **125**, 882–883.
5 B. Therrien, G. Suss-Fink, P. Govindaswamy, A. K. Renfrew and P. J. Dyson, *Angew. Chem., Int. Ed.*, 2008, **47**, 3773–3776.
6 M. M. Liu, Z. J. Lim, Y. Y. Gwee, A. Levina and P. A. Lay, *Angew. Chem., Int. Ed.*, 2010, **49**, 1661–1664.
7 L. Salassa, T. Ruiu, C. Garino, A. M. Pizarro, F. Bardelli, D. Gianolio, A. Westendorf, P. J. Bednarski, C. Lamberti, R. Gobetto and P. J. Sadler, *Organometallics*, 2010, **29**, 6703–6710.
8 M. D. Hall, G. J. Foran, M. Zhang, P. J. Beale and T. W. Hambley, *J. Am. Chem. Soc.*, 2003, **125**, 7524–7525.
9 T. Oida, Y. Sako and A. Kusumi, *Biophys. J.*, 1993, **64**, 676–685.
10 T. W. J. Gadella, T. M. Jovin and R. M. Clegg, *Biophys. Chem.*, 1993, **48**, 221–239.
11 E. B. van Munster and T. W. J. Gadella, *Adv. Biochem. Eng./Biotechnol.*, 2005, **95**, 143–175.
12 R. L. Arrowsmith, P. A. Waghorn, M. W. Jones, A. Bauman, S. K. Brayshaw, Z. Y. Hu, G. Kociok-Kohn, T. L. Mindt, R. M. Tyrrell, S. W. Botchway, J. R. Dilworth and S. I. Pascu, *Dalton Trans.*, 2011, **40**, 6238–6252.
13 P. A. Waghorn, M. W. Jones, M. B. M. Theobald, R. L. Arrowsmith, S. I. Pascu, S. W. Botchway, S. Faulkner and J. R. Dilworth, *Chem. Sci.*, 2013, **4**, 1430–1441.
14 G. Bar-Sela, R. Epelbaum and M. Schaffer, *Curr. Med. Chem.*, 2010, **17**, 190–197.
15 S. S. Bansal, M. Goel, F. Aqil, M. V. Vadhanam and R. C. Gupta, *Cancer Prev. Res.*, 2011, **4**, 1158–1171.
16 A. Castonguay, C. Doucet, M. Juhas and D. Maysinger, *J. Med. Chem.*, 2012, **55**, 8799–8806.
17 D. K. Agrawal and P. K. Mishra, *Med. Res. Rev.*, 2010, **30**, 818–860.
18 M. M. Yallapu, M. Jaggi and S. C. Chauhan, *Curr. Pharm. Des.*, 2013, **19**, 1994–2010.
19 F. Giannini, G. Suss-Fink and J. Furrer, *Inorg. Chem.*, 2011, **50**, 10552–10554.
20 F. Y. Wang, J. J. Xu, K. Wu, S. K. Weidt, C. L. Mackay, P. R. R. Langridge-Smith and P. J. Sadler, *Dalton Trans.*, 2013, **42**, 3188–3195.
21 M. D. Hall, T. W. Failes, N. Yamamoto and T. W. Hambley, *Dalton Trans.*, 2007, 3983–3990.
22 N. Yamamoto, S. Danos, P. D. Bonnitcha, T. W. Failes, E. J. New and T. W. Hambley, *JBIC, J. Biol. Inorg. Chem.*, 2008, **13**, 861–871.
23 T. W. Failes and T. W. Hambley, *Dalton Trans.*, 2006, 1895–1901.
24 T. W. Failes, C. Cullinane, C. I. Diakos, N. Yamamoto, J. G. Lyons and T. W. Hambley, *Chem.–Eur. J.*, 2007, **13**, 2974–2982.

25 W. H. Ang and P. J. Dyson, *Eur. J. Inorg. Chem.*, 2006, 4003–4018.
26 M. Sagnou, D. Benaki, C. Triantis, T. Tsotakos, V. Psycharis, C. P. Raptopoulou, I. Pirmettis, M. Papadopoulos and M. Pelecanou, *Inorg. Chem.*, 2011, **50**, 1295–1303.
27 K. Mohammadi, K. H. Thompson, B. O. Patrick, T. Storr, C. Martins, E. Polishchuk, V. G. Yuen, J. H. McNeill and C. Orvig, *J. Inorg. Biochem.*, 2005, **99**, 2217–2225.
28 S. Banerjee, P. Prasad, A. Hussain, I. Khan, P. Kondaiah and A. R. Chakravarty, *Chem. Commun.*, 2012, **48**, 7702–7704.
29 F. Caruso, M. Rossi, A. Benson, C. Opazo, D. Freedman, E. Monti, M. B. Gariboldi, J. Shaulky, F. Marchetti, R. Pettinari and C. Pettinari, *J. Med. Chem.*, 2012, **55**, 1072–1081.
30 F. Kuhlwein, K. Polborn and W. Beck, *Z. Anorg. Allg. Chem.*, 1997, **623**, 1211–1219.
31 T. Kojima, T. Amano, Y. Ishii, M. Ohba, Y. Okaue and Y. Matsuda, *Inorg. Chem.*, 1998, **37**, 4076–4085.
32 P. D. Bonnitcha, B. J. Kim, R. K. Hocking, J. K. Clegg, P. Turner, S. M. Neville and T. W. Hambley, *Dalton Trans.*, 2012, **41**, 11293–11304.
33 S. Dutta, A. Murugkar, N. Gandhe and S. Padhye, *Met.-Based Drugs*, 2001, **8**, 183–188.
34 A. Kunwar, S. K. Sandur, M. Krishna and K. I. Priyadarsini, *Eur. J. Pharmacol.*, 2009, **611**, 8–16.
35 S. W. Magennis, A. Habtemariam, O. Novakova, J. B. Henry, S. Meier, S. Parsons, I. D. H. Oswald, V. Brabec and P. J. Sadler, *Inorg. Chem.*, 2007, **46**, 5059–5068.
36 J. d. Mármol, O. Filevich and R. Etchenique, *Anal. Chem.*, 2010, **82**, 6259–6264.
37 H. Y. H. Ohori, M. Tomizawa, M. Shibuya, Y. Kakudo, A. Takahashi, S. Takahashi, S. Kato, T. Suzuki, C. Ishioka, Y. Iwabuchi and H. Shibata, *Mol. Cancer Ther.*, 2006, **5**, 2563–2571.
38 A. Habtemariam, M. Melchart, R. Fernández, S. Parsons, I. D. H. Oswald, A. Parkin, F. P. A. Fabbiani, J. E. Davidson, A. Dawson, R. E. Aird, D. I. Jodrell and P. J. Sadler, *J. Med. Chem.*, 2006, **49**, 6858–6868.
39 N. S. Bryce, J. Z. Zhang, R. M. Whan, N. Yamamoto and T. W. Hambley, *Chem. Commun.*, 2009, 2673–2675.
40 J. Z. Zhang, N. S. Bryce, R. Siegele, E. A. Carter, D. Paterson, M. D. d. Jonge, D. L. Howard, C. G. Ryan and T. W. Hambley, *Integr. Biol.*, 2012, **4**, 1072–1080.
41 A. Kunwar, A. Barik, B. Mishra, K. Rathinasamy, R. Pandey and K. I. Priyadarsini, *Biochim. Biophys. Acta, Gen. Subj.*, 2008, **1780**, 673–679.
42 B. J. Kim, T. W. Hambley and N. S. Bryce, *Chem. Sci.*, 2011, **2**, 2135–2142.
43 K. DeClerck and R. C. Elble, *Front. Biosci.*, 2010, **15**, 213–225.
44 T. J. S. A. Mukerjee, A. P. Ranjan, S. Raut, I. Gryczynski, J. K. Vishwanatha and Z. Gryczynski, *J. Phys. Chem. B*, 2010, **114**, 12679–12684.
45 R. Adhikary, P. Mukherjee, T. W. Kee and J. W. Petrich, *J. Phys. Chem. B*, 2009, **113**, 5255–5261.
46 M. F. A. Dutta, S. Roy, J. C. Schmitt, G. A. Hamilton, H. E. Hartnett, J. M. Shearer and A. K. Jones, *Inorg. Chem.*, 2013, **52**, 5236–5245.
47 P. D. Bonnitcha, M. D. Hall, C. K. Underwood, G. J. Foran, M. Zhang, P. J. Beale and T. W. Hambley, *J. Inorg. Biochem.*, 2006, **100**, 963–971.
48 M. D. Hall, C. K. Underwood, T. W. Failes, G. J. Foran and T. W. Hambley, *Aust. J. Chem.*, 2007, **60**, 180–183.
49 L. S. Kau, D. J. Spira-Solomon, J. E. Penner-Hahn, K. O. Hodgson and E. I. Solomon, *J. Am. Chem. Soc.*, 1987, **109**, 6433.